# GRAPHGAN: GENERATING GRAPHS VIA RANDOM WALKS

**Anonymous authors**
Paper under double-blind review

## ABSTRACT

We propose GraphGAN – the first implicit generative model for graphs that enables to mimic real-world networks. We pose the problem of graph generation as learning the distribution of biased random walks over a single input graph. Our model is based on a stochastic neural network that generates discrete output samples, and is trained using the Wasserstein GAN objective. GraphGAN enables us to generate *sibling graphs*, which have similar properties yet are not exact replicas of the original graph. Moreover, GraphGAN learns a semantic mapping from the latent input space to the generated graph's properties. We discover, that sampling from certain regions of the latent space leads to varying properties of the output graphs, with smooth transitions between them. Strong generalization properties of GraphGAN are highlighted by its competitive performance in link prediction and node classification, even though not specifically trained for these tasks.

## 1 INTRODUCTION

Generative models for graphs have a longstanding history, with applications including data augmentation, anomaly detection and recommendation (Chakrabarti & Faloutsos, 2006). *Explicit probabilistic models* such as Barabási-Albert or stochastic blockmodels are the de-facto standard in this field (Goldenberg et al., 2010). However, it has also been shown on multiple occasions that our intuitions about structure and behavior of graphs may be misleading. For instance, heavy-tailed degree distributions in real graphs were in stark disagreement with the models existing at the time of their discovery (Barabási & Albert, 1999). More recent works, like Dong et al. (2017), keep bringing up other surprising characteristics of real-world networks, not accounted for by the models at hand. This leads us to the question: "How do we define a model that captures all the essential (potentially still unknown) properties of real graphs?"

An increasingly popular way to address this issue in other fields is by switching from *explicit* (prescribed) models to *implicit* ones. This transition is especially notable in Computer Vision, where Variational Autoencoder (Kingma & Welling, 2013) and Generative Adversarial Networks (GANs) (Goodfellow et al., 2014) significantly advanced the state of the art over the classic prescribed approaches like Mixtures of Gaussians (Blanken et al., 2007). GANs achieve unparalleled results in scenarios such as image and 3D objects generation (e.g., Radford et al., 2015; Berthelot et al., 2017; Wu et al., 2016). However, despite their massive success when dealing with real-valued data, adapting GANs to handle *discrete* objects like graphs or text remains an open research problem (Goodfellow, 2016). Indeed, the combinatorial structure of the graph is only one of the obstacles when applying GANs to graphs. Second, large repositories of graphs, which all come from the same distribution, do not exist. This means that in a typical setting one has to learn from a *single graph*. And last, any model operating on a graph necessarily has to be *permutation invariant*, as the graphs remain isomorphic under node reordering.

In this work we introduce *GraphGAN* - the first implicit generative model for graphs, that tackles all of the above challenges. We formulate the problem of learning the graph topology as learning the distribution of biased random walks over the graph. Like in the typical GAN setting, the generator $G$ – in our case defined as a stochastic neural network with discrete output samples – learns to generate random walks that are *plausible* in the real graph, while the discriminator $D$ then has to distinguish them from the true ones, that are sampled from the original graph. The objective function of our model is based on the Wasserstein GAN (Arjovsky et al., 2017), which allows to

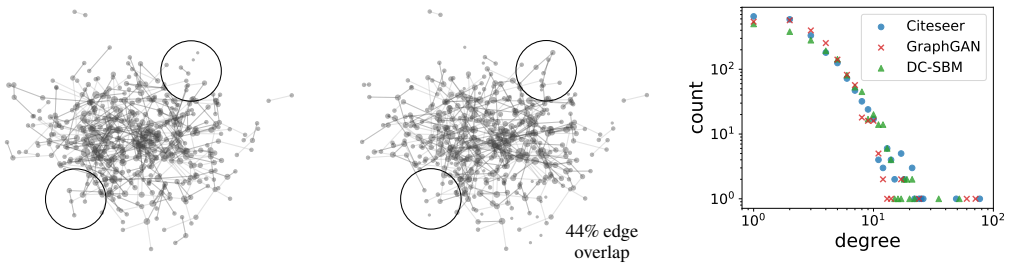


(a) Original graph (b) Sibling graph (c) Degree distribution comparison

Figure 1: GraphGAN is able to generate a *sibling graph* to the CITESEER network. (a) and (b) visualize a subset of nodes selected from the complete graphs. The graphs show similar structure but are not identical. (c) shows that the degree distributions of the input graph and of the graphs generated by GraphGAN and the degree-corrected stochastic blockmodel are very similar.

learn multimodal distributions and leads to more stable convergence. Our GraphGAN exhibits strong generalization properties, which we study in detail in the experimental section. The example in Figure 1 shows that the graphs generated by GraphGAN possess similar properties as the input graph, as shown by the degree distributions in Figure 1c. The generated graphs, however, are not simply exact replicas: as the visualized subset of nodes in Figures 1a and 1b shows, the graphs exhibit similar structure while being not identical; in fact, the two graphs have less than 50% of edges in common. This initial insight is underlined by an extensive comparison of graphs generated by GraphGAN and the respective input networks in the experimental section of this work. And even more, when generating graphs based on specific regions of the latent space learned by GraphGAN, we can smoothly interpolate between graphs with varying properties. Our main contributions are:

- We introduce *GraphGAN* - the first of its kind GAN that generates graphs via random walks. Our model tackles the associated challenges of staying permutation invariant, learning from a single graph and generating discrete output.
- We show that our model generalizes, and is able to produce *sibling graphs* to the given input graph. These graphs posses similar topological characteristics, but are not exact replicas (see Figure 1). We further demonstrate how latent space interpolation leads to generation of graphs with smoothly changing properties.
- We highlight the generalization properties of GraphGAN by its *link prediction* performance, which is competitive with the state of the art on real-word datasets, although not trained explicitly for this task. Additionally, our model learns meaningful *node embeddings* as a byproduct of the training process, that can be used for node classification.

## 2 RELATED WORK

There are only two attempts of using GANs in the context of graphs (Tavakoli et al., 2017; Liu et al., 2017). Tavakoli et al. (2017)'s approach tries to generate the full adjacency matrix of the graph directly (treating it as a binary image). To circumvent the issue of having a single graph, they apply random permutations to the adjacency matrix to generate additional training data. Since their model explicitly generates the full adjacency matrix – including zero-elements – the output (input) size of their generator (discriminator) is equal to the number of nodes squared. Such a quadratic complexity is infeasible in practice, allowing to process only small graphs. Indeed, this fundamental limitation becomes evident in their reported runtime of over 60 hours for a graph with only 154 nodes – the largest graph they processed. In contrast, our model operates on the random walks, thus only considering the non-zero elements of the adjacency matrix and efficiently exploiting the sparsity of real-wolrd graphs.

While not focusing on generating full graphs, Liu et al. (2017) use GANs to learn graph topological features. They decompose the graph into multiple subgraphs, where each subgraph is then processed by a GAN using standard image operations (e.g. convolution, deconvolution). Such operations,

however, assume spatial correlation, which does not apply in the graph setting: while the pixels in a local image patch are likely related, spatial correlation in a small patch of the adjacency matrix is generally not fulfilled due to the property of permutation invariance. Moreover, since their GAN only generates edges *within* the subgraphs, but not *between* them, all inter-subgraph edges from the original graph have to be stored and copied manually to a potential new graph. In contrast, our model is learned end-to-end, it allows to generate the whole graph, and it handles arbitrary permutations of the given input graph (since it is not based on spatial properties of the adjacency matrix).

Due to the challenging nature of the problem, only few approaches able to generate discrete data using GANs exist. Most approaches focus on generating discrete sequences such as text, with some of them using reinforcement learning techniques to address the difficulty of backpropagation through sampling discrete random variables (Yu et al., 2017; Kusner & Hernández-Lobato, 2016; Li et al., 2017; Liang et al., 2017). Other approaches modify the GAN objective to tackle the same challenge (Che et al., 2017; Hjelm et al., 2017). Focusing on non-sequential discrete data, Choi et al. (2017) generate high-dimensional discrete features (e.g. binary indicators, counts) in patient records. None of these methods has considered graph structured data.

Apart from GANs, prescribed generative models for graphs have a long history and are well-studied. For a comprehensive survey see Chakrabarti & Faloutsos (2006); Goldenberg et al. (2010). Based on the different modeling assumptions, the generative power of these models varies significantly. A substantial portion cannot even handle power-law degree distributions as found in most real-world networks. A strong representative able to capture such degree distributions, as well as diverse network topologies and community structure is the well-established degree-corrected stochastic blockmodel (DC-SBM) (Karrer & Newman, 2011). We compare against the DC-SBM as a baseline.

## 3 GANs FOR GRAPHS

In this section we introduce *GraphGAN* - a Generative Adversarial Network model for graphs. Its core idea lies in learning the topology of a graph by learning the distribution over the random walks. Given is an input graph of $N$ nodes, defined by an unweighted adjacency matrix $\boldsymbol{A} \in \{0,1\}^{N \times N}$. First, we sample a set of random walks of length $T$ from $\boldsymbol{A}$. This collection of random walks serves as a training set for our model. We use the biased second-order random walk sampling strategy described in Grover & Leskovec (2016), as it better captures both local and global graph structure. An important advantage of using random walks is their invariance under node reordering. Additionally, random walks only include the nonzero entries of $\boldsymbol{A}$, thus efficiently exploiting the sparsity of real-world graphs.

Like any typical GAN architecture, GraphGAN consists of two main components - a generator $G$ and a discriminator $D$. The goal of the generator is to generate synthetic random walks that are *plausible* in the input graph. At the same time, the discriminator learns to distinguish the synthetic random walks from the real ones, that come from the training set. Both $G$ and $D$ are trained end-to-end using backpropagation. At any point of the training process it is possible to use $G$ to generate a set of random walks, which can then be used to produce an adjacency matrix of a new generated graph. In the rest of this section we describe each stage of this process and our design choices in more detail. An overview of our model's complete architecture can be seen in Figure 2.

### 3.1 ARCHITECTURE

**Generator.** The generator $G$ defines an implicit probabilistic model for generating the random walks: $(\boldsymbol{v}_1, ..., \boldsymbol{v}_T) \sim G$. We model $G$ as a sequential process based on a neural network $f_\theta$ parametrized by $\theta$. At each step $t$, $f_\theta$ produces two values: the probability distribution over the next node to be sampled, denoted as $\boldsymbol{p}_t$, and the current *memory state* of the model, denoted as $\boldsymbol{m}_t$. The new node $\boldsymbol{v}_t$ (represented as a one-hot vector) is sampled from $\mathrm{Cat}(\boldsymbol{p}_t)$, and together with $\boldsymbol{m}_t$ passed into $f_\theta$ at the next step

$$
\begin{aligned}
& & \boldsymbol{z} &\sim \mathcal{N}(\boldsymbol{0}, \boldsymbol{I}_d) \\
& & \boldsymbol{m}_0 &= g_{\theta'}(\boldsymbol{z}) \\
\boldsymbol{v}_1 &\sim \mathrm{Cat}(\boldsymbol{p}_1), & (\boldsymbol{p}_1, \boldsymbol{m}_1) &= f_\theta(\boldsymbol{m}_0, \boldsymbol{0}) \\
\boldsymbol{v}_2 &\sim \mathrm{Cat}(\boldsymbol{p}_2), & (\boldsymbol{p}_2, \boldsymbol{m}_2) &= f_\theta(\boldsymbol{m}_1, \boldsymbol{v}_1) \\
\vdots & & \vdots & \\
\boldsymbol{v}_T &\sim \mathrm{Cat}(\boldsymbol{p}_T), & (\boldsymbol{p}_T, \boldsymbol{m}_T) &= f_\theta(\boldsymbol{m}_{T-1}, \boldsymbol{v}_{T-1})
\end{aligned}
$$

$t+1$. Similarly to the classic GAN setting, a latent code $\boldsymbol{z}$ drawn from a multivariate standard normal distribution is passed through a parametric function $g_{\theta'}$ to initialize $\boldsymbol{m}_0$. The generative process of $G$ is summarized in the box above.

In this work we focus our attention on the Long short-term memory (LSTM) architecture for $f_\theta$, introduced by Hochreiter & Schmidhuber (1997). The memory state $\boldsymbol{m}_t$ of an LSTM is represented by the cell state $\boldsymbol{C}_t$, and the hidden state $\boldsymbol{h}_t$. The latent code $\boldsymbol{z}$ goes through two separate streams, each consisting of two fully connected layers with $\tanh$ activation, and then used to initialize $(\boldsymbol{C}_0, \boldsymbol{h}_0)$.

A natural question might arise: "Why use a model with memory and temporal dependencies, when the random walks are Markov processes?" (2nd order Markov for biased RWs). Or put differently, what's the benefit of using random walks of length greater than 2. In theory, a model with large enough capacity could simply memorize all existing edges in the graph and recreate them. However, for large graphs achieving this in practice is not feasible. More importantly, pure memorization is not the goal of GraphGAN, rather we want to have generalization and generate similar sibling graphs, not exact replicas. Having longer random walks combined with memory helps the model to learn the topology and general patterns in the data (e.g. community structure). Our experiments in Sec. 4.2 confirm this, showing that longer random walks are indeed beneficial.

After each time step, in order to generate the next node in the random walk, the network $f_\theta$ needs to output the vector of probabilities $\boldsymbol{p}_t$ of length $N$. Operating in such high dimensional space within the LSTM cell is infeasible, and leads to unnecessary computational overhead. For this reason, we do the following: the model outputs $\boldsymbol{o}_t \in \mathbb{R}^H$, with $H \ll N$, which is then projected up to $\mathbb{R}^N$ using the *context embedding matrix* $\boldsymbol{W}_{up} \in \mathbb{R}^{N \times H}$.

Given the probability distribution over the next node in the random walk, $\boldsymbol{p}_t \in \Delta^{N-1}$, from which $\boldsymbol{v}_t$ is to be drawn, we are faced with another challenge: Sampling from a categorical distribution is a non-differentiable operation – thus, it blocks the flow of gradients and precludes backpropagation. We circumvent this problem by using the Gumbel-Softmax estimator from Jang et al. (2016). More specifically, we perform the following transformation: First, we let $\boldsymbol{v}_t^* = \text{softmax}\left(\frac{\log \boldsymbol{p}_t + \boldsymbol{g}}{\tau}\right)$, where $\tau$ is a temperature parameter, and $g_i$'s are i.i.d. samples from a Gumbel distribution with zero mean and unit scale. Then, the next sample is computed as $\boldsymbol{v}_t = \text{onehot}(\arg\max \boldsymbol{v}_t^*)$. While the one-hot sample $\boldsymbol{v}_t$ is passed as input to the next time step, during the backward pass the gradients will flow through the differentiable $\boldsymbol{v}_t^*$. The choice of $\tau$ allows to trade-off between better flow of gradients (large $\tau$, more uniform $\boldsymbol{v}_t^*$) and more exact calculations (small $\tau$, $\boldsymbol{v}_t^* \approx \boldsymbol{v}_t$).

Now, that a new node $\boldsymbol{v}_t$ is sampled, it needs to be projected back to a lower-dimensional representation before feeding into the LSTM. This is done by means of the *embedding matrix* $\boldsymbol{W}_{down} \in \mathbb{R}^{H \times N}$. Together with the context embedding matrix $\boldsymbol{W}_{up}$, the matrix $\boldsymbol{W}_{down}$ deserves a special mention, as it happens to learn – as a byproduct – meaningful embeddings for the nodes, that can be used for other tasks. We study properties of these embeddings in Sec. 4.3.

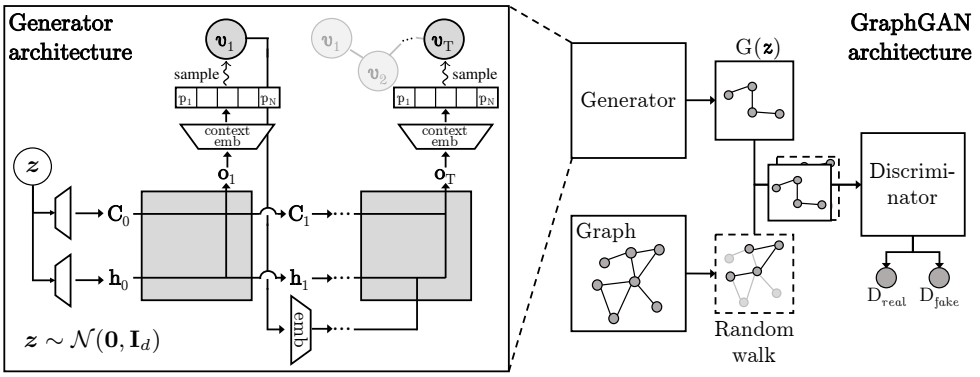


(a) (b)

Figure 2: The GraphGAN architecture proposed in this work (b) and the generator architecture (a). *emb* denotes projection of the one-hot nodes into low-dimensional embedding space, while *context emb* denotes projection of low-dimensional space into dimension $N$.

**Discriminator.** The discriminator $D$ is based on the standard LSTM architecture. At every time step $t$, a one-hot vector $\boldsymbol{v}_t$, denoting the node at the current position, is fed as input. After processing the entire sequence, the discriminator outputs a single score that represents the probability of the random walk being real.

### 3.2 TRAINING

**Wasserstein GAN.** We train our model based on the Wasserstein GAN (WGAN) framework (Arjovsky et al., 2017). To enforce the Lipschitz constraint of the discriminator, we use the gradient penalty as in Gulrajani et al. (2017). We observe, that in our setting using the WGAN objective leads to noticeable improvements over the vanilla GAN: it prevents mode collapse, as well as leads to a more stable learning procedure overall. The model parameters $\{\theta, \theta'\}$ are trained using stochastic gradient descent with Adam (Kingma & Ba, 2014). Weights are regularized with an $L_2$ penalty.

**Early stopping.** Because we are interested in generalizing the input graph, the "trivial" solution where the generator has memorized all existing edges is of no interest to us. This means that we need to control overfitting of our model. To achieve this, we employ two early stopping strategies. The first strategy, named VAL-CRITERION is concerned with the generalization properties of GraphGAN. During training, we keep a sliding window of the random walks generated in the last 1,000 iterations and use them to construct a matrix of transition counts. This matrix is then used to evaluate the link prediction performance on a validation set (i.e. ROC and AP scores, for more details see Sec. 4.2). We stop with training when the validation performance stops improving.

The second strategy, named EO-CRITERION makes GraphGAN very flexible and gives the user control over the graph generation. We stop with training when we achieve a user specified edge overlap between the generated graphs (see next section) and the original one at a given iteration. Based on her end task the user can choose to generate graphs with either small or large edge overlap with the original, while maintaining structural similarity. This will lead to generated graphs that either generalize more or are closer replicas respectively, yet still capture the properties of the original.

### 3.3 ASSEMBLING THE ADJACENCY MATRIX

After finishing the training, we use the generator $G$ to construct a score matrix $\boldsymbol{S}$ of transition counts, i.e. we count often an edge appeared in the set of generated random walks (typically, using a much larger number of random walks than for early stopping, e.g., 500K). While the raw counts matrix $\boldsymbol{S}$ is sufficient for link prediction purposes, we need to convert it to a binary adjacency matrix $\tilde{\boldsymbol{A}}$, if we wish to reason about the synthetic graph. First, $\boldsymbol{S}$ is symmetrized by setting $s_{ij} = s_{ji} = \max\{s_{ij}, s_{ji}\}$. Because we cannot explicitly control for the starting node of the random walks generated by $G$, some high-degree nodes will likely be overrepresented. Thus, a simple binarization strategy like thresholding or choosing top-$k$ entries might lead to leaving out the low-degree nodes and producing singletons. To address this issue, we use the following approach. (i) We ensure that every node $i$ has at least one edge by sampling a neighbor $j$ with probability $p_{ij} = \frac{s_{ij}}{\sum_v s_{iv}}$. If an edge was already sampled before, we repeat the procedure. (ii) We continue sampling edges without replacement, using for each edge $(i, j)$ the probability $p_{ij} = \frac{s_{ij}}{\sum_{u,v} s_{uv}}$, until we reach the desired amount of edges (e.g., as many edges as in the original graph). Note, that this procedure is not guaranteed to produce a fully connected graph.

## 4 EXPERIMENTS

Besides using GraphGAN to generate graphs, we also evaluate its output and learned representations on other typical graph mining tasks, most prominently link prediction and node classification. We evaluate GraphGAN on these tasks and several real-world datasets and compare it with state-of-the-art methods. Furthermore, we demonstrate how we can generate graphs with smoothly changing properties via latent space interpolation.

**Datasets.** For our evaluation, we use several well-know citation datasets, as well as the Political Blogs dataset. Table 1 show the dataset statistics. Cora-ML is the subset of machine learning papers from the original Cora dataset typically considered in other works. For all our experiments, we consider only the largest connected component in each network and treat them as undirected.

Table 1: Dataset statistics

| | Pol. Blogs | Cora-ML (McCallum et al., 2000) | Cora (Giles et al., 1998) | Citeseer (Sen et al., 2008) | Pubmed (Pan et al., 2016) | DBLP |
|---|---|---|---|---|---|---|
| Number of nodes | 1490 | 2,995 | 19,793 | 3,312 | 19,717 | 17,716 |
| Largest conn. comp. size | 1,222 | 2,810 | 18,800 | 2,110 | 19,717 | 16,191 |
| Number of edges | 19,025 | 8,416 | 65,311 | 4,715 | 44,324 | 52,867 |
| Edges in LCC | 16,714 | 8,229 | 64,529 | 3,757 | 44,324 | 51,913 |
| Number of communities | 2 | 7 | 70 | 6 | 3 | 4 |

Table 2: Comparison of graph statistics between the original CORA-ML graph and graphs generated by GraphGAN and DC-SBM, averaged over 5 trials. Marked in bold and italic are the results that are closest and second-closest to the input graph, respectively.

| **Graph** | **Max. degree** | | **Assortativity** | | **Triangle count** | | **Power law exponent** | | **Largest conn. comp.** | | **Edge overlap** | |
|---|---|---|---|---|---|---|---|---|---|---|---|---|
| | Avg. | Std. | Avg. | Std. | Avg. | Std. | Avg. | Std. | Avg. | Std. | Avg. | Std. |
| CORA-ML | 240 | | -0.075 | | 2,814 | | 1.86 | | 2,810 | | | |
| GraphGAN VAL-CRITERION | *199* | ± 6.7 | *-0.060* | ± 0.004 | *1,410* | ± 30 | 1.773 | ± 0.002 | **2,809** | ± 1.6 | 39% | ± 0.004 |
| GraphGAN EO-CRITERION | **233** | ± 3.6 | **-0.066** | ± 0.003 | **1,588** | ± 59 | *1.793* | ± 0.003 | *2,807* | ± 1.6 | .52 | ± 0.001 |
| DC-SBM | 165 | ± 9.0 | -0.052 | ± 0.004 | 1,403 | ± 67 | **1.814** | ± 0.008 | 2,474 | ± 18.9 | 0.11 | ± 0.003 |

### 4.1 GRAPH GENERATION

In this task, we use GraphGAN to generate *sibling graphs* to a given input graph, and compare its performance to DC-SBM. The goal is to generate graphs that are similar in their properties to the input graph – while not trivially copying the input network. We randomly hide 15% of the edges (which are used for the stopping criterion; see Sec. 3.2) and train GraphGAN and DC-SBM on the remaining graph. We then sample graphs from the trained models and compare their properties with the input graph. We report here the results for CORA-ML, and for CITESEER in the appendix.

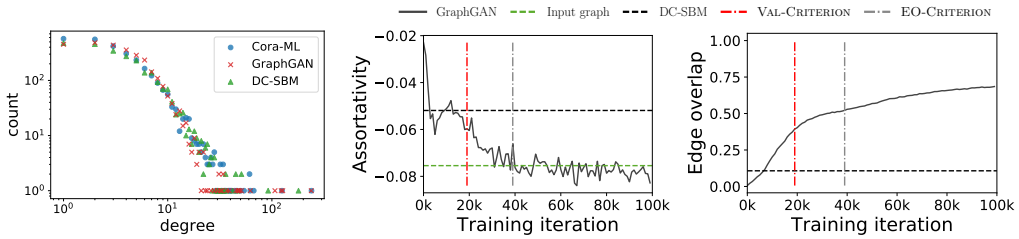


(a) Degree distribution

(b) Assortativity over training iterations

(c) Edge overlap (EO) over training iterations

Figure 3: Properties of generated graphs, trained on CORA-ML.

**Evaluation.** Figure 3a shows that GraphGAN and DC-SBM are able to generate graphs whose degree distributions nicely match the input graph's. For DC-SBM, this is not surprising, given that it *explicitly* encodes the degree distribution in the model. GraphGAN, however, does not have access to the degree distribution of the input graph – yet is still able to model it to a high accuracy. Going beyond the degree distribution, in Table 2 we show five other important graph statistics and see that for most of them GraphGAN is closer to the original graph compared to DC-SBM. We report the results for both early stopping strategies: VAL-CRITERION and EO-CRITERION. In line with our intuition, we can see that higher EO leads to generated graphs with closer statistics to the original. For even more statistics, as well as all of their definitions, see the appendix.

Figures 3b and 3c show how the graph statistics evolve as we train GraphGAN on CORA-ML. In Fig. 3b we see that after 40K training iterations we are able to reach the assortativity value of the original graph. Fig. 3c shows that the edge overlap smoothly increasing with the number of epochs. Note: EO is a suitable measure of closeness since we generate graphs with same number of edges as the input. We provide similar plots for the other graph statistics and for CITESEER in the appendix.

### 4.2 LINK PREDICTION

Link prediction is a classical task in graph mining, where the goal is to predict new links in a given graph. We use it to evaluate the generalization properties of GraphGAN. We hold out 10% of edges from the graph for validation, and 5% as the test set, along with the same amount of randomly selected non-edges. We also ensure that the training network remains connected and does not contain any singletons. We measure the performance with the commonly used metrics ROC area-under-curve (AUC) score and precision-recall AUC score, known as average precision (AP).

To evaluate GraphGAN's link prediction performance, we sample a specific number of random walks from the trained generator. We use the observed transition counts between any two nodes as a measure of how likely there is an edge between them. Additionally, we concatenate the learned node and context embeddings and use the dot product as an alternative way to perform link prediction. We compare with Adamic/Adar (Adamic & Adar, 2003), the degree-corrected stochastic blockmodel (DC-SBM) (Karrer & Newman, 2011), and node2vec (Grover & Leskovec, 2016).

**Evaluation.** The results are listed in Table 3. There is no overall dominating method, with different methods achieving best results on different datasets. GraphGAN shows competitive performance for all datasets, for both the transition count based and the embedding based link prediction, even achieving state-of-the-art results for some of them, despite not being explicitly trained for this task.

Table 3: Link prediction performance. For GraphGAN (100M) and GraphGAN (500K) we sampled the corresponding number of random walks from the trained model for evaluation. (emb.) indicates link prediction performance when using the embeddings learned by GraphGAN.

| **Method** | CORA-ML | | CORA | | CITESEER | | DBLP | | PUBMED | | POLBLOGS | |
|---|---|---|---|---|---|---|---|---|---|---|---|---|
| | ROC | AP | ROC | AP | ROC | AP | ROC | AP | ROC | AP | ROC | AP |
| Adamic/Adar | 92.16 | 85.43 | 93.00 | 86.18 | 88.69 | 77.82 | 91.13 | 82.48 | 84.98 | 70.14 | 85.43 | 92.16 |
| DC-SBM | **96.03** | 95.15 | 98.01 | 97.45 | 94.77 | 93.13 | **97.05** | **96.57** | **96.76** | 95.64 | 95.46 | **94.93** |
| node2vec | 92.19 | 91.76 | **98.52** | **98.36** | 95.29 | 94.58 | 96.41 | 96.36 | 96.49 | **95.97** | 85.10 | 83.54 |
| GraphGAN (500K) | 94.00 | 92.32 | 82.31 | 68.47 | 95.18 | 91.93 | 82.45 | 70.28 | 87.39 | 76.55 | 95.06 | 94.61 |
| GraphGAN (100M) | 95.19 | **95.24** | 84.82 | 88.04 | **96.30** | **96.89** | 86.61 | 89.21 | 93.41 | 94.59 | **95.51** | 94.83 |
| GraphGAN (emb.) | 90.29 | 88.29 | 84.38 | 79.36 | 92.95 | 92.44 | 86.59 | 81.96 | 91.79 | 89.37 | 70.01 | 62.72 |

Interestingly, for the transition count based link prediction, the GraphGAN performance increases when increasing the number of random walks sampled from the generator. This is especially true for the larger networks (CORA, DBLP, PUBMED), since given their size we need more random walks to cover the entire graph. This suggests that for an additional computational cost, one can get significant gains in performance. Note that while 100M may seem like an large number, the sampling process is trivially parallelizable.

**Sensitivity analysis.** Althogh GraphGAN has many hyper-parameters – typical for a GAN model, in practice most of them are not critical for performance. The two important exceptions are the length of the random walks $T$, and the discriminator type. Figure 4 empirically confirms the choice of a neural network that generates random walks of length $T$ as opposed to just edges; the model does not have the capacity to fit the model by just considering edges (i.e. random walks of length 2). The performance gain for random walk length 20 over 16 is marginal and does not outweigh the additional computational cost; for all experiments, we therefore trained GraphGAN on random walks of length 16. In the appendix we show that our choice of a recurrent discriminator achieves better link prediction performance than a variant based on convolutions, hence we use it for all experiments in this work.

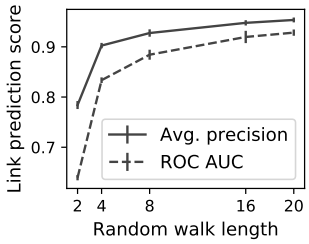


Figure 4: Sensitivity analysis. Evaluation via sampling 500K random walks from the trained models; for each configuration, five separate models were trained.

### 4.3 NODE CLASSIFICATION

We perform node classification using the learned embeddings to show the generalization properties of GraphGAN. We evaluate both the regular embeddings $\boldsymbol{W}_{down}$, the context embeddings $\boldsymbol{W}_{up}$, as well as their combination, comparing with node2vec as a strong baseline. Note that unlike the

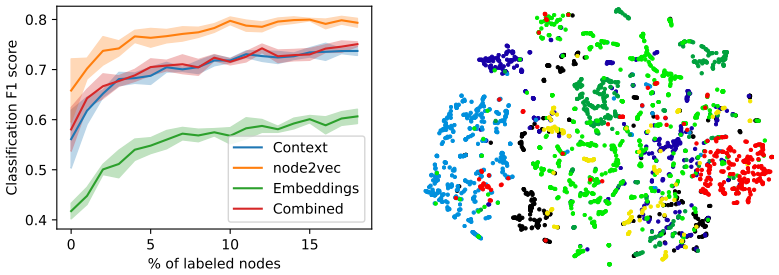


(a) (b)

Figure 5: (a) Node classification performance on CORA-ML for different node embeddings, and (b) t-SNE visualization of context embeddings, where the color indicates the ground truth communities.

link prediction task we cannot use the generated graph to perform node classification. Similar to (Grover & Leskovec, 2016; Perozzi et al., 2014) we train a logistic regression model on a small randomly selected subset ($< 20\%$ of nodes) using the ground-truth labels and evaluate the classification performance on the remaining samples. Additionally, we visualize the embeddings using t-SNE to demonstrate that a community structure has emerged in the embedding space.

**Evaluation.** In Figure 5a, we visualize the weighted macro F1 score for node classification. The results are averaged over five trials, and the shaded areas indicate the standard deviation of the respective curves. The embeddings produced by GraphGAN as a byproduct show competitive performance with node2vec – an algorithm specifically designed to learn useful node embedding. This indicates that during the process of learning to generate random walks GraphGAN also learned meaningful node embeddings. Figure 5b further emphasizes this. In this t-SNE visualization of the context embeddings learned by GraphGAN, we can clearly see a grouping of nodes from the same community, which means that they lie in similar regions of the embedding space. Interestingly, the context embeddings outperform the regular node embeddings by a surprisingly large margin, which may be a starting point for follow-up research. Although GraphGAN's learned embedding clearly show they they capture useful information about the nodes, they are only a byproduct of the training procedure. The main goal of GraphGAN is graph generation, if node classification is the user goal, dedicated node embedding algorithms are better suited.

### 4.4 LATENT VARIABLE INTERPOLATION

Latent space interpolation is a good way to gain insight into what kind of structure the generator was able to capture. To be able to visualize the properties of the generated graphs we train our model with only two dimensions of unit Gaussian noise as the input. Then instead of sampling from the entire latent space $\boldsymbol{z}$, we now sample from subregions and visualize the results. More specifically, we use the inverse of the cumulative distribution $\Phi(p(\boldsymbol{z}))$ to divide the two-dimensional latent space $\Omega$ into $20 \times 20$ bins of equal probability mass and generate 62.5K random walks per bin from our model. We evaluate properties of both the generated random walks themselves, as well as properties of the resulting graph when sampling a binary adjacency matrix for each bin, visualizing them as heatmaps.

**Evaluation.** In Figure 6 we see some statistics of the generated random walks on CORA-ML within their respective bins. In Fig. 6a and 6b we see properties of the generated random walks; in Fig. 6c and 6d, we visualize properties of graphs sampled from the random walks in the respective bins. In all four heatmaps, we see distinct patterns, e.g. higher average degree of starting nodes for the bottom right region of Fig. 6a, or higher degree distribution inequality in the top-right area of Fig. 6c. While Figure 6c and 6d, show that certain regions of $\boldsymbol{z}$ correspond to generated graphs with very different degree distributions, recall that sampling from the entire latent space ($\Omega$) yields *sibling* graphs with degree distribution similar to the original graph (see Fig. 1c). We provide further heatmaps for other metrics (16 in total) as well as visualizations for CITESEER in the appendix.

This experiment clearly demonstrates that by interpolating in the latent space we can obtain graphs with smoothly changing properties. The smooth transitions in the heatmaps provide evidence that our model learns to map specific parts of the latent space to specific properties of the graph.

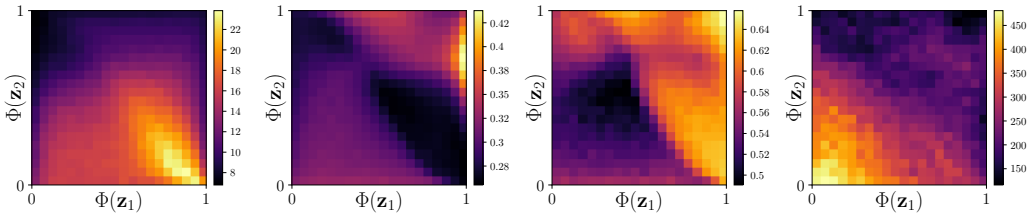


(a) Avg. degree of start node

(b) Avg. share of nodes in start community

(c) Gini coefficient (input graph: 0.48)

(d) Max. degree (input graph: 240)

Figure 6: Properties of the random walks as well as the graphs sampled from the $20 \times 20$ bins. 6a and 6b show properties of the random walks, 6c and 6d show properties of the generated graphs.

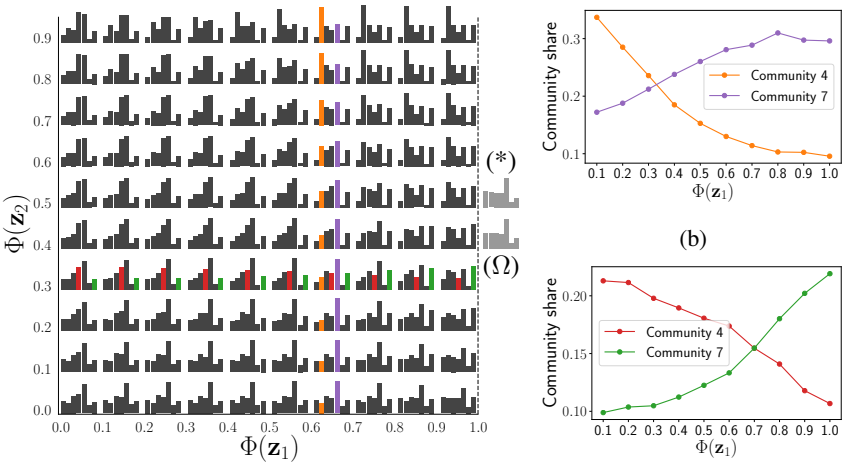


(a) Community histograms

(b)

(c)

Figure 7: Community distributions (see appendix for definition) when sampling random walks on subsets of the latent space $\boldsymbol{z}$. (a) shows complete community histograms on a $10 \times 10$ grid. (b) and (c) show exemplary trajectories in latent space. ($\Omega$) is the community distribution when sampling from the complete latent space, and (*) is the community distribution of the CORA-ML network.

We can also see this mapping from latent space to the generated graph properties in the community distribution histograms on a $10 \times 10$ grid in Fig. 7. Marked by (*) and ($\Omega$) we see the community distributions for the input graph and the graph obtained by sampling on the complete latent space, respectively. In Fig. 7b and 7c, we see the evolution of selected community shares when following a trajectory from top to bottom, and left to right, respectively. The community histograms resulting from sampling random walks from opposing regions of the latent space are very different; again the transitions between these histograms are smooth, as can be seen in the trajectories in Fig. 7b and 7c.

## 5 DISCUSSION AND FUTURE WORK

Being the first model of its kind, GraphGAN opens numerous avenues for future work.

**Other types of data.** While plain graphs are ubiquitous, many of real-world applications deal with attributed, k-partite or heterogeneous networks. Adapting the GraphGAN model to handle these other modalities of the data is a promising direction for future research. Especially important would be an adaptation to the dynamic / inductive setting, when new nodes are added over time.

**Scalability.** There are multiple directions in which the GraphGAN model can be improved to permit scaling to massive graphs (100K+ nodes). We have observed in Sec. 4.2, that it takes a large number of generated random walks to get representative transition counts for large graphs. While sampling random walks from GraphGAN is trivially parallelizable, a possible extension of our model is to use

a *conditional* generator, i.e. the generator can be provided a desired starting node, thus ensuring an even coverage. On the other hand, the sampling procedure itself can be sped up by incorporating a hierarchical softmax output layer - a method commonly used in natural language processing.

**Evaluation measures.** It is nearly impossible to judge whether a graph is *realistic* by visually inspecting it (unlike images, for example). In this work we already used a number of standard graph properties to quantitatively evaluate performance of our model. However, such metrics might not be optimal for the given problem. Developing new measures will allow us to more fairly evaluate competing methods, and better understand the behavior of generative graph models.

## 6 CONCLUSION

GraphGAN is the first work to successfully bridge the worlds of implicit modeling and graphs. Our work enables future researchers to gain better insight into the properties of real networks and opens new and exciting lines of research. We are able to generate realistic graphs by learning to generate (biased) random walks from the same distribution as the random walks from an input graph. We employ the GAN framework to learn our implicit generative model, overcoming key challenges such as permutation invariance, working in the discrete domain and having a single graph as input. Our generator is able to generate sibling graphs that maintain structural similarity with the original graph without being exact replicas. Better yet, using our defined stopping criteria, we can control how close are the generated graphs to the original. We further show that GraphGAN learns a semantic mapping from the latent space to the properties of the generated graph, which is evidenced by the smooth transitions of the output. GraphGAN shows strong generalization properties, as demonstrated by the competitive performance on the link prediction and node classification tasks, without being explicitly trained with these tasks in mind.

## REFERENCES

Lada A Adamic and Eytan Adar. Friends and neighbors on the web. *Social networks*, 25(3):211–230, 2003.

Martin Arjovsky, Soumith Chintala, and Léon Bottou. Wasserstein gan. *arXiv preprint arXiv:1701.07875*, 2017.

Albert-László Barabási and Réka Albert. Emergence of scaling in random networks. *science*, 286 (5439):509–512, 1999.

David Berthelot, Tom Schumm, and Luke Metz. Began: Boundary equilibrium generative adversarial networks. *arXiv preprint arXiv:1703.10717*, 2017.

Henk M Blanken, Arjen P de Vries, Henk Ernst Blok, and Ling Feng. *Multimedia retrieval*. Springer, 2007.

Deepayan Chakrabarti and Christos Faloutsos. Graph mining: Laws, generators, and algorithms. *ACM computing surveys (CSUR)*, 38(1):2, 2006.

Tong Che, Yanran Li, Ruixiang Zhang, R Devon Hjelm, Wenjie Li, Yangqiu Song, and Yoshua Bengio. Maximum-likelihood augmented discrete generative adversarial networks. *arXiv preprint arXiv:1702.07983*, 2017.

Edward Choi, Siddharth Biswal, Bradley Malin, Jon Duke, Walter F Stewart, and Jimeng Sun. Generating multi-label discrete electronic health records using generative adversarial networks. *arXiv preprint arXiv:1703.06490*, 2017.

Yuxiao Dong, Reid A Johnson, Jian Xu, and Nitesh V Chawla. Structural diversity and homophily: A study across more than one hundred big networks. In *Proceedings of the 23rd ACM SIGKDD International Conference on Knowledge Discovery and Data Mining*, pp. 807–816. ACM, 2017.

C Lee Giles, Kurt D Bollacker, and Steve Lawrence. Citeseer: An automatic citation indexing system. In *Proceedings of the third ACM conference on Digital libraries*, pp. 89–98. ACM, 1998.

Anna Goldenberg, Alice X Zheng, Stephen E Fienberg, Edoardo M Airoldi, et al. A survey of statistical network models. *Foundations and Trends® in Machine Learning*, 2(2):129–233, 2010.

Ian Goodfellow. Nips 2016 tutorial: Generative adversarial networks. *arXiv preprint arXiv:1701.00160*, 2016.

Ian Goodfellow, Jean Pouget-Abadie, Mehdi Mirza, Bing Xu, David Warde-Farley, Sherjil Ozair, Aaron Courville, and Yoshua Bengio. Generative adversarial nets. In *Advances in neural information processing systems*, pp. 2672–2680, 2014.

Aditya Grover and Jure Leskovec. node2vec: Scalable feature learning for networks. In *Proceedings of the 22nd ACM SIGKDD international conference on Knowledge discovery and data mining*, pp. 855–864. ACM, 2016.

Ishaan Gulrajani, Faruk Ahmed, Martin Arjovsky, Vincent Dumoulin, and Aaron Courville. Improved training of wasserstein gans. *arXiv preprint arXiv:1704.00028*, 2017.

R Devon Hjelm, Athul Paul Jacob, Tong Che, Kyunghyun Cho, and Yoshua Bengio. Boundary-seeking generative adversarial networks. *arXiv preprint arXiv:1702.08431*, 2017.

Sepp Hochreiter and Jürgen Schmidhuber. Long short-term memory. *Neural Computation*, 9 (8):1735–1780, 1997. doi: 10.1162/neco.1997.9.8.1735. URL `http://dx.doi.org/10.1162/neco.1997.9.8.1735`.

Eric Jang, Shixiang Gu, and Ben Poole. Categorical reparameterization with gumbel-softmax. *arXiv preprint arXiv:1611.01144*, 2016.

Brian Karrer and Mark EJ Newman. Stochastic blockmodels and community structure in networks. *Physical Review E*, 83(1):016107, 2011.

Diederik Kingma and Jimmy Ba. Adam: A method for stochastic optimization. *arXiv preprint arXiv:1412.6980*, 2014.

Diederik P Kingma and Max Welling. Auto-encoding variational bayes. *arXiv preprint arXiv:1312.6114*, 2013.

Matt J Kusner and José Miguel Hernández-Lobato. Gans for sequences of discrete elements with the gumbel-softmax distribution. *arXiv preprint arXiv:1611.04051*, 2016.

Jiwei Li, Will Monroe, Tianlin Shi, Alan Ritter, and Dan Jurafsky. Adversarial learning for neural dialogue generation. *arXiv preprint arXiv:1701.06547*, 2017.

Xiaodan Liang, Zhiting Hu, Hao Zhang, Chuang Gan, and Eric P Xing. Recurrent topic-transition gan for visual paragraph generation. *arXiv preprint arXiv:1703.07022*, 2017.

Weiyi Liu, Pin-Yu Chen, Hal Cooper, Min Hwan Oh, Sailung Yeung, and Toyotaro Suzumura. Can gan learn topological features of a graph? *arXiv preprint arXiv:1707.06197*, 2017.

Andrew Kachites McCallum, Kamal Nigam, Jason Rennie, and Kristie Seymore. Automating the construction of internet portals with machine learning. *Information Retrieval*, 3(2):127–163, 2000.

Shirui Pan, Jia Wu, Xingquan Zhu, Chengqi Zhang, and Yang Wang. Tri-party deep network representation. *Network*, 11(9):12, 2016.

Bryan Perozzi, Rami Al-Rfou, and Steven Skiena. Deepwalk: Online learning of social representations. In *Proceedings of the 20th ACM SIGKDD international conference on Knowledge discovery and data mining*, pp. 701–710. ACM, 2014.

Alec Radford, Luke Metz, and Soumith Chintala. Unsupervised representation learning with deep convolutional generative adversarial networks. *arXiv preprint arXiv:1511.06434*, 2015.

Prithviraj Sen, Galileo Namata, Mustafa Bilgic, Lise Getoor, Brian Galligher, and Tina Eliassi-Rad. Collective classification in network data. *AI magazine*, 29(3):93, 2008.

Sahar Tavakoli, Alireza Hajibagheri, and Gita Sukthankar. Learning social graph topologies using generative adversarial neural networks. 2017.

Jiajun Wu, Chengkai Zhang, Tianfan Xue, Bill Freeman, and Josh Tenenbaum. Learning a probabilistic latent space of object shapes via 3d generative-adversarial modeling. In *Advances in Neural Information Processing Systems*, pp. 82–90, 2016.

Lantao Yu, Weinan Zhang, Jun Wang, and Yong Yu. Seqgan: Sequence generative adversarial nets with policy gradient. In *AAAI*, pp. 2852–2858, 2017.

## APPENDIX

We denote as $V$ the set of all nodes in a graph, $E$ as the set of edges, and as $C_i \subseteq V, i \in \{1, \ldots, k\}$ communities in a graph. Every node in the graphs we consider is assigned to exactly one of these communities. $N(v) = \{v' | (v, v') \in E\}$ denotes the set of neighbors of a node $v$, and $d(v) = |N(v)|$ is the degree of node $v$.

Given two graphs $G_1$ and $G_2$ with the same number of nodes and edges, i.e. $|V_1| = |V_2|$, $|E_1| = |E_2|$, we define their *edge overlap* as

$$\text{EO}(G_1, G_2) = \frac{|E_1 \cap E_2|}{|E_1|} = \frac{|E_1 \cap E_2|}{|E_2|}.$$

Table 4: Graph statistics used to measure graph properties in this work.

| **Metric name** | **Computation** | **Description** |
|---|---|---|
| Maximum degree | $\max_{v \in V} d(v)$ | Maximum degree of all nodes in a graph. |
| Community distribution | $c_i = \frac{\sum_{v \in C_i} d(v)}{\sum_{v \in V} d(v)}$ | Share of in- and outgoing edges of community $C_i$, normalized by the number of edges in the graph. |
| LCC | $N_{max} = \max_{f \subseteq F} \lvert f \rvert$ | Size of largest connected component, where $F$ are all connected components. |
| Power law exponent | $1 + n \left( \sum_{u \in V} \log \frac{d(u)}{d_{\min}} \right)^{-1}$ | Exponent of the power law distribution, where $d_{min}$ denotes the minimum degree in a network. |
| Gini coefficient | $\frac{2 \sum_{i=1}^{\lvert V \rvert} i \hat{d}_i}{\lvert V \rvert \sum_{i=1}^{\lvert V \rvert} \hat{d}_i} - \frac{\lvert V \rvert + 1}{\lvert V \rvert}$ | Common measure for inequality in a distribution, where $\hat{\boldsymbol{d}}$ is the sorted list of degrees in the graph. |
| Triangle count | $\frac{\lvert \{\{u,v,w\} \mid \{(u,v),(v,w),(u,w)\} \subseteq E\} \rvert}{6}$ | Number of triangles in the graph, where $u \sim v$ denotes that $u$ and $v$ are connected. |
| Wedge count | $\sum_{v \in V} \binom{d(v)}{2}$ | Number of wedges, i.e. two-hop paths in an undirected graph. |
| Rel. edge distr. entropy | $\frac{1}{\ln \lvert V \rvert} \sum_{v \in V} -\frac{d(v)}{\lvert E \rvert} \ln \frac{d(v)}{\lvert E \rvert}$ | Entropy of degree distribution, 1 means uniform, 0 means a single node is connected to all others. |
| Assortativity | $\rho = \frac{\text{cov}(X,Y)}{\sigma_X \sigma_Y}$ | Pearson correlation of degrees of connected nodes, where the $(x_i, y_i)$ pairs are the degrees of connected nodes. |

Table 5: GraphGAN with recurrent vs convolutional discriminator. We train GraphGAN with the recurrent and convolutional discriminator variants five times each and measure their link prediction scores on the CORA-ML dataset to evaluate which variant is suited better for our task.

| **Discri-** | **ROC AUC** | | **Avg. Prec.** | |
|---|---|---|---|---|
| **minator** | Mean | Std. | Mean | Std |
| Recurrent | **92.07** | $\pm$ 0.005 | **94.88** | $\pm$ 0.002 |
| Conv. | 89.70 | $\pm$ 0.017 | 93.02 | $\pm$ 0.011 |

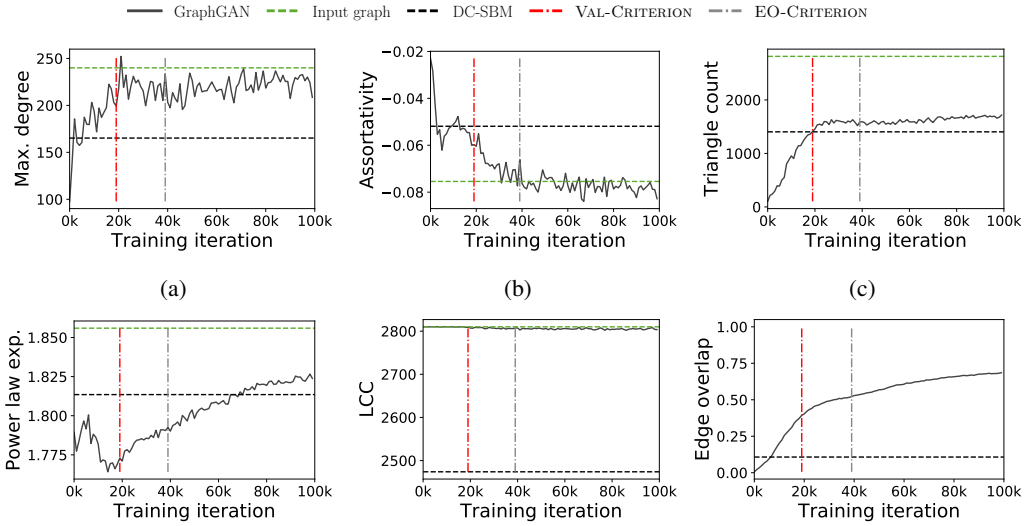


Figure 8: Evolution of graph statistics during training on CORA-ML

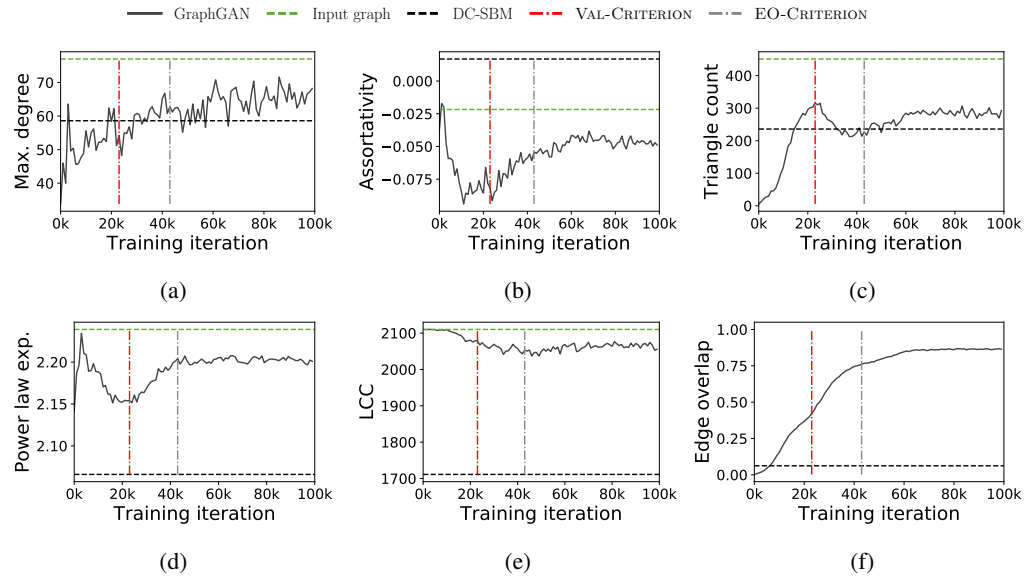


Figure 9: Evolution of graph statistics during training on CITESEER

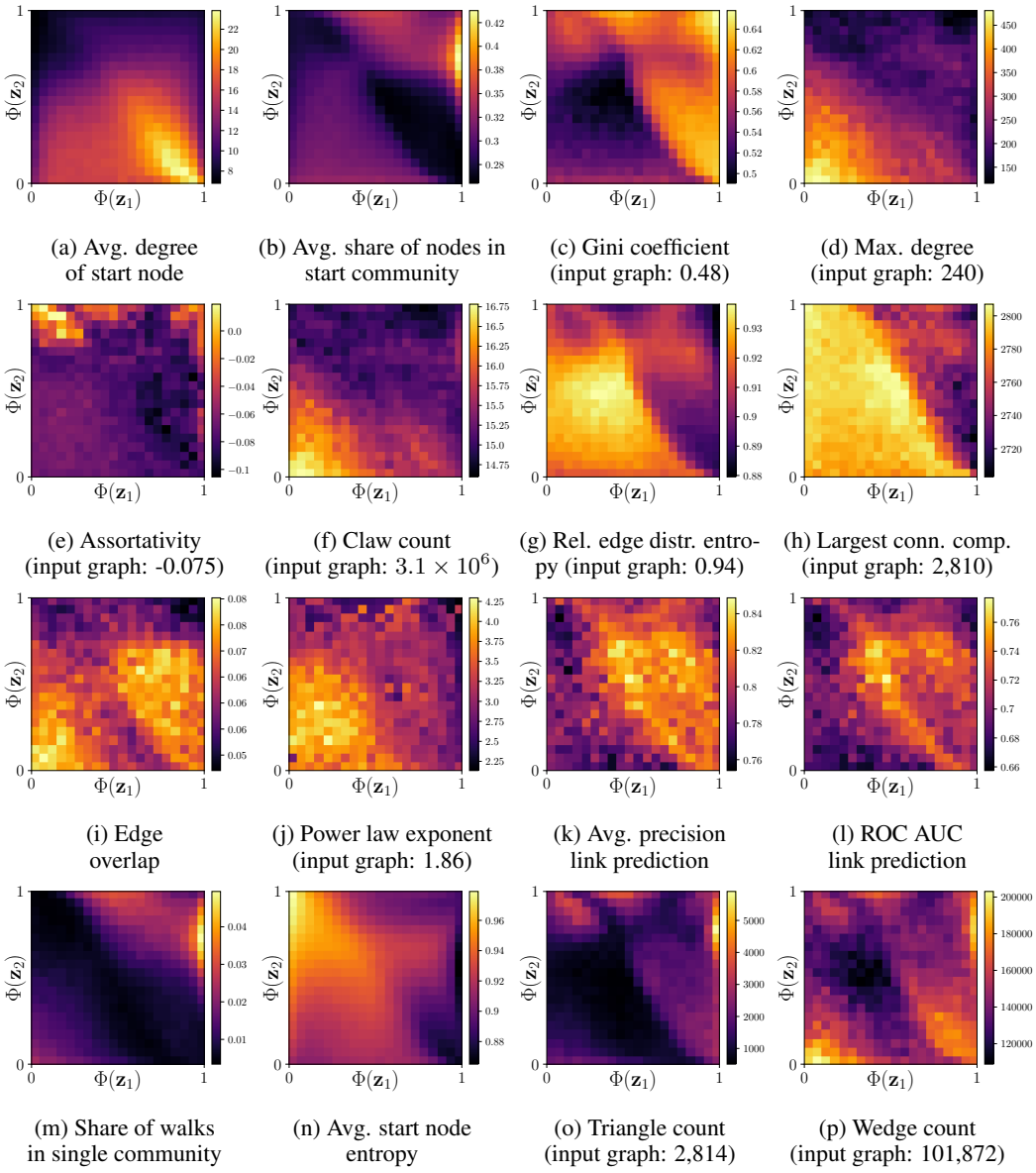


(a) Avg. degree of start node

(b) Avg. share of nodes in start community

(c) Gini coefficient (input graph: 0.48)

(d) Max. degree (input graph: 240)

(e) Assortativity (input graph: -0.075)

(f) Claw count (input graph: $3.1 \times 10^6$)

(g) Rel. edge distr. entropy (input graph: 0.94)

(h) Largest conn. comp. (input graph: 2,810)

(i) Edge overlap

(j) Power law exponent (input graph: 1.86)

(k) Avg. precision link prediction

(l) ROC AUC link prediction

(m) Share of walks in single community

(n) Avg. start node entropy

(o) Triangle count (input graph: 2,814)

(p) Wedge count (input graph: 101,872)

Figure 10: Properties of the random walks as well as the graphs sampled from the $20 \times 20$ latent space bins, trained on CORA-ML.

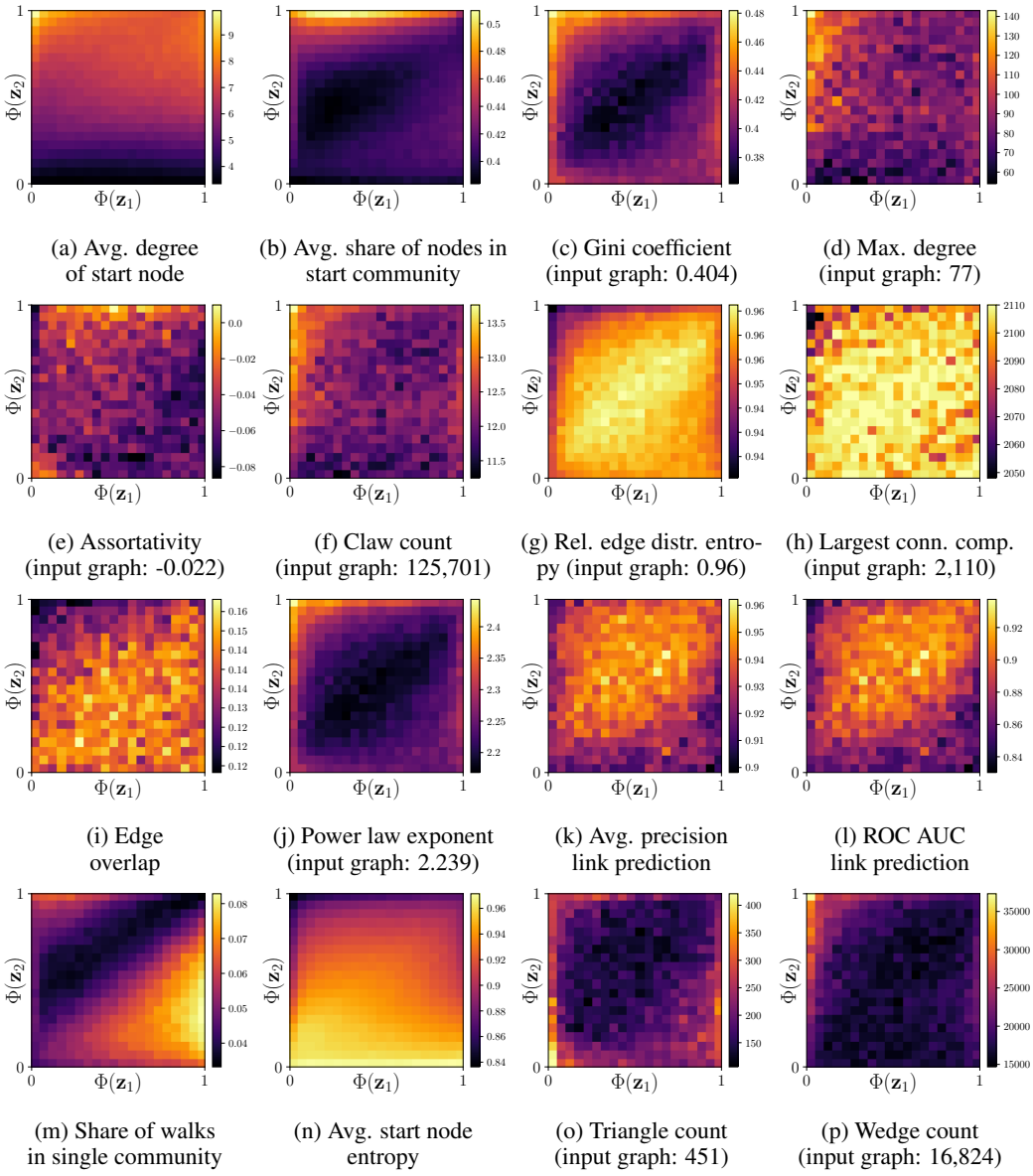


(a) Avg. degree of start node
(b) Avg. share of nodes in start community
(c) Gini coefficient (input graph: 0.404)
(d) Max. degree (input graph: 77)
(e) Assortativity (input graph: -0.022)
(f) Claw count (input graph: 125,701)
(g) Rel. edge distr. entropy (input graph: 0.96)
(h) Largest conn. comp. (input graph: 2,110)
(i) Edge overlap
(j) Power law exponent (input graph: 2.239)
(k) Avg. precision link prediction
(l) ROC AUC link prediction
(m) Share of walks in single community
(n) Avg. start node entropy
(o) Triangle count (input graph: 451)
(p) Wedge count (input graph: 16,824)

Figure 11: Properties of the random walks as well as the graphs sampled from the $20 \times 20$ latent space bins, trained on CITESEER.

Table 6: Comparison of graph statistics between the CITESEER/CORA-ML graph and graphs generated by GraphGAN and DC-SBM, averaged after 5 trials. Marked in bold and italic are the results that are closest and second-closest to the ground truth graph, respectively, except for edge overlap, where lower can be considered better.

| **Graph** | **Max. degree** | | **Assortativity** | | **Triangle count** | | **Power law exponent** | | **Edge overlap** | |
|---|---|---|---|---|---|---|---|---|---|---|
| | Avg. | Std. | Avg. | Std. | Avg. | Std. | Avg. | Std. | Avg. | Std. |
| CITESEER | 77 | | -0.022 | | 451 | | 2.239 | | 1 | |
| GraphGAN (42% EO) | *54* | ± 4.2 | -0.082 | ± 0.009 | **316** | ± 11.2 | *2.154* | ± 0.003 | *0.42* | ± 0.006 |
| GraphGAN (76% EO) | **63** | ± 4.3 | **-0.054** | ± 0.006 | 227 | ± 13.3 | **2.204** | ± 0.003 | 0.76 | ± 0.01 |
| DC-SBM (6.6% EO) | 53 | ± 5.6 | *0.022* | ± 0.018 | *257* | ± 30.9 | 2.066 | ± 0.014 | **0.066** | ± 0.011 |
| CORA-ML | 240 | | -0.075 | | 2,814 | | 1.86 | | 1 | |
| GraphGAN (39% EO) | *199* | ± 6.7 | *-0.060* | ± 0.004 | *1,410* | ± 30 | 1.773 | ± 0.002 | *0.39* | ± 0.004 |
| GraphGAN (52% EO) | **233** | ± 3.6 | **-0.066** | ± 0.003 | **1,588** | ± 59 | *1.793* | ± 0.003 | 0.52 | ± 0.001 |
| DC-SBM (11% EO) | 165 | ± 9.0 | -0.052 | ± 0.004 | 1,403 | ± 67 | **1.814** | ± 0.008 | **0.11** | ± 0.003 |

| **Graph** | **Wedge count** | | **Rel. edge distr. entr.** | | **Largest conn. comp** | | **Claw count** | | **Gini coeff.** | |
|---|---|---|---|---|---|---|---|---|---|---|
| | Avg. | Std. | Avg. | Std. | Avg. | Std. | Avg. | Std. | Avg. | Std. |
| CITESEER | 16,824 | | 0.959 | | 2,110 | | 125,701 | | 0.404 | |
| GraphGAN (42% EO) | 12,998 | ± 84.6 | *0.969* | ± 0.000 | **2,079** | ± 12.6 | 57,654 | ± 4,226 | *0.354* | ± 0.001 |
| GraphGAN (76% EO) | *15,202* | ± 378 | **0.963** | ± 0.000 | *2,053* | ± 23 | **94,149** | ± 11,926 | **0.385** | ± 0.002 |
| DC-SBM (6.6% EO) | **15,531** | ± 592 | 0.938 | ± 0.001 | 1,697 | ± 27.049 | *69,818* | ± 11,969 | 0.502 | ± 0.005 |
| CORA-ML | 101,872 | | 0.941 | | 2,810 | | $3.1 \cdot 10^6$ | | 0.482 | |
| GraphGAN (39% EO) | *75,724* | ± 1,401 | 0.959 | ± 0.000 | **2,809** | ± 1.6 | $\mathit{1.8 \cdot 10^6}$ | ± 141,795 | 0.398 | ± 0.002 |
| GraphGAN (52% EO) | **86,763** | ± 1,096 | *0.954* | ± 0.001 | *2,807* | ± 1.6 | $\mathbf{2.6 \cdot 10^6}$ | ± 103,667 | *0.42* | ± 0.003 |
| DC-SBM (11% EO) | 73,921 | ± 3,436 | **0.934** | ± 0.001 | 2,474 | ± 18.9 | $1.2 \cdot 10^6$ | ± 170,045 | **0.523** | ± 0.003 |

Figure 12: Community distributions of graphs generated by GraphGAN on subregions of the latent space $\boldsymbol{z}$, trained on the CITESEER network.